

Original Paper

Ca²⁺/Calmodulin Binding to STIM1 Hydrophobic Residues Facilitates Slow Ca²⁺-Dependent Inactivation of the Orai1 Channel

Rajesh Bhardwaj^{a,b} Bartłomiej S. Augustynek^{a,b} Ebru Ercan-Herbst^{c,d}
Palanivel Kandasamy^{a,b} Matthias Seedorf^d Christine Peinelt^e
Matthias A. Hediger^{a,b}

^aMembrane Transport Discovery Lab, Department of Nephrology and Hypertension, Inselspital Bern, Bern, Switzerland, ^bDepartment of Biomedical Research, University of Bern, Bern, Switzerland, ^cBioMed X Innovation Center, Heidelberg, Germany, ^dCenter for Molecular Biology, University of Heidelberg, Heidelberg, Germany, ^eInstitute of Biochemistry and Molecular Medicine, University of Bern, Bern, Switzerland

Key Words

STIM1 • SOCE • I_{CRAC} • SCDI • Calmodulin • Orai1

Abstract

Background/Aims: Store-operated Ca²⁺ entry (SOCE) through plasma membrane Ca²⁺ channel Orai1 is essential for many cellular processes. SOCE, activated by ER Ca²⁺ store-depletion, relies on the gating function of STIM1 Orai1-activating region SOAR of the ER-anchored Ca²⁺-sensing protein STIM1. Electrophysiologically, SOCE is characterized as Ca²⁺ release-activated Ca²⁺ current (I_{CRAC}). A major regulatory mechanism that prevents deleterious Ca²⁺ overload is the slow Ca²⁺-dependent inactivation (SCDI) of I_{CRAC}. Several studies have suggested a role of Ca²⁺/calmodulin (Ca²⁺/CaM) in triggering SCDI. However, a direct contribution of STIM1 in regulating Ca²⁺/CaM-mediated SCDI of I_{CRAC} is as yet unclear. **Methods:** The Ca²⁺/CaM binding to STIM1 was tested by pulling down recombinant GFP-tagged human STIM1 C-terminal fragments on CaM sepharose beads. STIM1 was knocked out by CRISPR/Cas9 technique in HEK293 cells stably overexpressing human Orai1. Store-operated Ca²⁺ influx was measured using Fluorometric Imaging Plate Reader and whole-cell patch clamp in cells transfected with STIM1 CaM binding mutants. The involvement of Ca²⁺/CaM in SCDI was investigated by including recombinant human CaM in patch pipette in electrophysiology. **Results:** Here we identified residues Leu³⁷⁴/Val³⁷⁵ (H1) and Leu³⁹⁰/Phe³⁹¹ (H2) within SOAR that serve as hydrophobic anchor sites for Ca²⁺/CaM binding. The bifunctional H2 site is critical for both

R. Bhardwaj and B. S. Augustynek contributed equally to this work as first authors. C. Peinelt and M. A. Hediger contributed equally to this work as last authors.

Matthias A. Hediger and
Rajesh Bhardwaj

Membrane Transport Discovery Lab, Department of Nephrology and Hypertension, Inselspital, University of Bern, Kinderklinik, Office D845, Freiburgstrasse 15, CH-3010 Bern (Switzerland)
Tel. +41 31 632 94 39 (Office), +41 31 632 22 93 (Lab),
E-Mail matthias.hediger@ibmm.unibe.ch; rajesh.bhardwaj@dbmr.unibe.ch

Orai1 activation and Ca²⁺/CaM binding. Single residue mutations of Phe³⁹¹ to less hydrophobic residues significantly diminished SOCE and I_{CRAC}, independent of Ca²⁺/CaM. Hence, the role of H2 residues in Ca²⁺/CaM-mediated SCDI cannot be precisely evaluated. In contrast, the H1 site controls exclusively Ca²⁺/CaM binding and subsequently SCDI, but not Orai1 activation. V375A but not V375W substitution eliminated SCDI of I_{CRAC} caused by Ca²⁺/CaM, proving a direct role of STIM1 in coordinating SCDI. **Conclusion:** Taken together, we propose a mechanistic model, wherein binding of Ca²⁺/CaM to STIM1 hydrophobic anchor residues, H1 and H2, triggers SCDI by disrupting the functional interaction between STIM1 and Orai1. Our findings reveal how STIM1, Orai1, and Ca²⁺/CaM are functionally coordinated to control I_{CRAC}.

© 2020 The Author(s). Published by
Cell Physiol Biochem Press GmbH&Co. KG

Introduction

Calcium (Ca²⁺) regulates a wide array of physiological functions in eukaryotic cells. The endoplasmic reticulum (ER) is the major intracellular Ca²⁺ store and, upon its depletion, e.g. through activation of IP₃ receptors, a refilling process known as store-operated calcium entry (SOCE) is initiated [1]. SOCE relies on ER-anchored luminal Ca²⁺-sensing STIM proteins (STIM1 and STIM2), and Orai Ca²⁺ channels (Orai1, Orai2 and Orai3) in the plasma membrane (PM), with STIM1 and Orai1 playing a predominant role in most cell types [1-5]. Following ER Ca²⁺ store depletion, STIM1 proteins undergo conformational changes and oligomerization, leading to exposure of different STIM1 domains [6-14]. STIM1 proteins are targeted to PI(4,5)P₂ anchored in the inner leaflet of the PM via their C-terminal lysine (K)-rich domain, resulting in a physical coupling of ER and PM [13, 15, 16]. The STIM1 Orai1-activating region SOAR activates Ca²⁺-selective Orai1 channels in the PM [17], leading to influx of Ca²⁺ that is electrophysiologically characterized as Ca²⁺ release-activated Ca²⁺ current (I_{CRAC}) [18]. CRAC channel-mediated Ca²⁺ influx is essential for the acute refilling of ER Ca²⁺ stores [19], as well as for the activation of multiple Ca²⁺-dependent downstream effectors such as NFAT [1, 20-22]. STIM1-mediated Orai1 activation mechanisms have been widely studied in the past decade [23, 24]. STIM2 has a similar function in gating Orai1 but responds to smaller decreases in ER Ca²⁺ concentrations [25, 26].

Following CRAC channel activation, regulation of I_{CRAC} is critically important to maintain Ca²⁺ homeostasis and to prevent deleterious intracellular Ca²⁺ overload. CRAC channel inactivation is known to be triggered by the elevation of cytosolic Ca²⁺ [27, 28]. Two spatiotemporally distinct Ca²⁺-dependent inactivation (CDI) mechanisms, namely slow Ca²⁺-dependent inactivation (SCDI) and fast Ca²⁺-dependent inactivation (FCDI), jointly control Ca²⁺ entry through CRAC channels [29, 30]. Both SCDI and FCDI regulate the activation of Ca²⁺ dependent transcription factors [31, 32]. FCDI develops over milliseconds and is reduced upon whole cell dialysis with high concentrations of the rapid Ca²⁺ buffer BAPTA but is unaffected by the slower Ca²⁺ buffer EGTA which has at least 100 times lower Ca²⁺ on- and off-rates [33, 34]. SCDI, on the other hand, develops over tens of seconds and requires a global rise in cytosolic Ca²⁺. SCDI is suppressed upon whole cell dialysis with high concentrations of either BAPTA or EGTA [27, 28]. In various cell types, the rate and extent of SCDI is modulated by mitochondrial Ca²⁺ buffering [35-39]. In addition, STIM1-associated ER membrane protein (SARAF) has been reported to facilitate both SCDI and FCDI of CRAC channels [40-43]. In resting cells, the C-terminal inhibitory domain (CTID) of STIM1 (residues 448-530) implicated in both SCDI [40] and FCDI [44-46], facilitates the interaction of SARAF with SOAR and prevents the spontaneous activation of STIM1. Store depletion causes an initial dissociation of SARAF from SOAR to allow CRAC channel activation. Subsequently, CTID-assisted reassociation of SARAF with SOAR has been proposed as a mechanism for SARAF-mediated SCDI of CRAC channels [40].

It is well-known that the ubiquitous Ca²⁺ sensor calmodulin (CaM) upon binding of cytosolic Ca²⁺ (Ca²⁺/CaM) undergoes a conformational change and exposes hydrophobic protein binding regions. Ca²⁺/CaM binds to numerous proteins and modulates various functions [47, 48]. Ca²⁺/CaM plays fundamentally important regulatory roles in numerous

ion channels including triggering of CDI [49]. Dysfunctions in Ca²⁺/CaM based regulatory mechanisms are linked to several human diseases [49-52]. The key components of the CRAC machinery, STIM1 and Orai1 channel proteins have been shown to interact with Ca²⁺/CaM [16, 46, 53-60]. However, Ca²⁺/CaM, STIM1 and Orai1 interaction sites and the underlying regulatory mechanism of SCDI still remain unclear. Initially, it was suggested that binding of Ca²⁺/CaM to the N-terminus of Orai1 (residues Y80 and W76) regulates the FCDI of CRAC channels [46]. Yet, it was shown that these Orai1 residues enable conformational changes within the pore, leading to CRAC channel inactivation without the requirement of Ca²⁺/CaM [59]. STIM1 K-rich domain binds Ca²⁺/CaM and is required for the STIM1-SARAF interaction as well as for SARAF-mediated SCDI of I_{CRAC} [43] [16, 54]. Deletion of the K-rich domain of STIM1 led to only a small decrease in Ca²⁺/CaM binding, suggesting that there are likely additional Ca²⁺/CaM binding motifs in STIM1 [16]. Recently, it was shown that Leu³⁹⁰/Phe³⁹¹ residues in SOAR interact with Ca²⁺/CaM [61]. Substituting Leu³⁹⁰/Phe³⁹¹ with serines diminished binding of Ca²⁺/CaM to STIM1 but also Orai1 activation independent of Ca²⁺/CaM [61].

Our previous in silico analysis of STIM1 amino acid sequence on CaM-target database server suggested the presence of a CaM binding domain within SOAR (CaMBD_{SOAR}, residues 372-394). We showed that within the CaMBD_{SOAR} both H1 (Leu³⁷⁴/Val³⁷⁵) and H2 (Leu³⁹⁰/Phe³⁹¹) hydrophobic residue sites are crucial for binding of Ca²⁺/CaM to STIM1. Based on these findings, we hypothesized that STIM1 H1/H2 site(s) play a role in Ca²⁺/CaM-mediated SCDI of CRAC channels. Mutation of H2 residues or only Phe³⁹¹ directly interfered with Orai1 activation independently of Ca²⁺/CaM, preventing precise SCDI analysis. In contrast, H1 is dispensable for Orai1 activation but critical for Ca²⁺/CaM binding. Substitution of Val³⁷⁵ in H1 to alanine eliminates Ca²⁺/CaM-mediated SCDI of I_{CRAC}, whereas substitution to tryptophan retains Ca²⁺/CaM-mediated SCDI. Our findings therefore provide a direct functional link between association of Ca²⁺/CaM to STIM1 and SCDI of CRAC channels, and segregate the roles of H1 and H2 residues of STIM1 in Orai1 activation and slow Ca²⁺-dependent Ca²⁺/CaM-mediated inactivation.

Materials and Methods

Plasmids

Bacterial expression and purification constructs: The bacterial expression and purification pET15b construct carrying the N-terminally 6X-His-GFP tagged cytosolic part of human STIM1 [15] was modified by site-directed mutagenesis (SDM) to generate a construct encoding for protein lacking the C-terminal K (lysine)-rich domain [16]. A stop codon (TAG) was introduced after residue position 670 of STIM1 by SDM using 5'-GAC TCC AGC CCA GGC TAG CGG AAG AAG TTT CCT-3' forward and 5'-AGG AAA CTT CTT CCG CTA GCC TGG GCT GGA GTC-3' reverse primers. Thus, obtained N-terminally 6X-His-GFP tagged cytosolic part of hSTIM1 lacking the K-rich domain (STIM1CT-ΔK) construct was further modified by SDM to mutagenize the H1 and H2 hydrophobic positions in hSTIM1 putative Ca²⁺/CaM binding domain. The Leu³⁹⁰ and Phe³⁹¹ residues were both mutated to alanine (H2AA) in the STIM1CT-ΔK pET15b construct by SDM using 5'-AAG AAG AGA AAC ACA GCC GCT GGC ACC TTC CAC GTG-3' forward and 5'-CAC GTG GAA GGT GCC AGC GGC TGT GTT TCT CTT CTT-3' reverse primers. Leu³⁷⁴ and Val³⁷⁵ were both mutated to alanine (H1AA) in the STIM1CT-ΔK pET15b construct by SDM using 5'-GCT GAG AAG CAG CTG GCG GCG GCC AAG GAG GGG GCT-3' forward and 5'-AGC CCC CTC CTT GGC CGC CGC CTG CTT CTC AGC-3' reverse primers. Similarly, the H1AA substitutions were also performed in the STIM1CT-ΔK H2AA construct in order to combine the H1AA and H2AA mutations in the STIM1CT-ΔK pET15b construct.

In order to remove the Ca²⁺/CaM binding domain completely from the STIM1CT-ΔK pET15b construct, first, an additional PmlI restriction site was engineered by SDM after K371 residue of STIM1 using 5'-CAA AAT GCT GAG AAG CAC GTG CTG GTG GCC AAG GAG-3' forward and 5'-CTC CTT GGC CAC CAG CAC GTG CTT CTC AGC ATT TTG-3' reverse primers. Another PmlI restriction site was already present in the construct after F394 residue of STIM1. The PmlI digested construct, after removal of the 69 bp fragment, was

extracted by gel purification and ligated using T4 DNA ligase (NEB). This resulted into a 7.719 kB STIM1CT-ΔK ΔCaMBD_{SOAR} pET15b construct where STIM1 residues 372-394 were removed.

Mammalian expression constructs: The HA-hSTIM1 peGFP-N1 construct [62] was modified by inserting mCherry after the HA-tag to create the HA-mCherry-hSTIM1 construct (STIM1). mCherry was amplified from the pmCherry-N1 construct kindly provided by Dr. Holger Lorenz (University of Heidelberg, Germany) using the 5'-ATA TAA GCT TGC ACC GGT CGC CAC CAT GGT GAG CAA GGG C-3' forward and 5'-ATA TAA GCT TGG AGC CTG CGT ACA AAC TTG TTG ATC CGG ACT TGT ACA GCT CGT CCA TGC CGC CGG-3' reverse primers. The obtained PCR product with 5' and 3' HindIII restriction site overhangs was digested with HindIII enzyme and ligated into the HindIII digested HA-hSTIM1 peGFP-N1 vector. In the same manner, the HA-hSTIM2 peGFP-N1 construct [62] was modified by inserting mCherry after the HA-tag to create the HA-mCherry-hSTIM2 construct (STIM2). Both HA-mCherry-hSTIM1 and HA-mCherry-hSTIM2 constructs contained the signal sequence of hSTIM1 just upstream of the HA-tag.

The HA-mCherry (control) plasmid was constructed by introducing a stop codon after mCherry in the HA-mCherry-hSTIM1 peGFP-N1 construct by SDM using 5'-GCA TGG ACG AGC TGT ACA AGT AGG GAT CAA CAA GTT TGT ACG CAG-3' forward and 5'-CTG CGT ACA AAC TTG TTG ATC CCT ACT TGT ACA GCT CGT CCA TGC-3' reverse primers. The control plasmid also contained the signal sequence of hSTIM1 just upstream of the HA-tag.

The Leu³⁹⁰ and Phe³⁹¹ residues were both mutated to alanine in HA-mCherry-hSTIM1 peGFP-N1 construct by SDM using 5'-GAT AAA AAA GAA GAG AAA CAC AGC CGC TGG CAC CTT CCA CGT GGC CCA C-3' forward and 5'-GTG GGC CAC GTG GAA GGT GCC AGC GGC TGT GTT TCT CTT CTT TTT TAT C-3' reverse primers to generate HA-mCherry-hSTIM1-H2AA peGFP-N1 construct (STIM1 H2AA). The V394 and F395 residues were both mutated to alanine in HA-mCherry-hSTIM2 peGFP-N1 construct by SDM using 5'-TTA AAA AGA AGA GAA GCA CAG CCG CTG GGA CTC TGC ACG TTG CAC A-3' forward and 5'-TGT GCA ACG TGC AGA GTC CCA GCG GCT GTG CTT CTC TTC TTT TTA A-3' reverse primers to generate HA-mCherry-hSTIM2-H2AA peGFP-N1 construct (STIM2 H2AA).

The C-terminal K-rich domain deletion mutant of HA-mCherry-hSTIM1 in peGFP-N1 was constructed by inserting a stop codon before the last 15 residues of hSTIM1 in the construct by SDM using 5'-GAC TCC AGC CCA GGC TAG CGG AAG AAG TTT CC-3' forward and 5'-GGA AAC TTC TTC CGC TAG CCT GGG CTG GAG TC-3' reverse primers (STIM1-ΔK). F391W substitution in the STIM1-ΔK construct was made by SDM using 5'-GAA GAG AAA CAC ACT CTG GGG CAC CTT CCA CGT GGC-3' forward and 5'-GCC ACG TGG AAG GTG CCC CAG AGT GTG TTT CTC TTC-3' reverse primers. F391L substitution in the STIM1-ΔK construct was made by SDM using 5'-GAA GAG AAA CAC ACT CCT GGG CAC CTT CCA CGT G-3' forward and 5'-CAC GTG GAA GGT GCC CAG GAG TGT GTT TCT CTT C-3' reverse primers. F391V substitution in the STIM1-ΔK construct was made by SDM using 5'-GAA GAG AAA CAC ACT CGT TGG CAC CTT CCA CGT G-3' forward and 5'-CAC GTG GAA GGT GCC AAC GAG TGT GTT TCT CTT C-3' reverse primers. F391A substitution in the STIM1-ΔK construct was made by SDM using 5'-GAA GAG AAA CAC ACT CGC TGG CAC CTT CCA CGT G-3' forward and 5'-CAC GTG GAA GGT GCC AGC GAG TGT GTT TCT CTT C-3' reverse primers. The H2AA (L374A-V375A) substitutions in STIM1 as well as STIM1-ΔK constructs were performed by SDM using the same primer pair mentioned above in the bacterial expression and purification constructs. In STIM1-ΔK construct, Val³⁷⁵ of STIM1 was mutagenized to tryptophan by SDM using 5'-GCT GAG AAG CAG CTG CTG TGG GCC AAG GAG GGG GCT GAG-3' forward and 5'-CTC AGC CCC CTC CTT GGC CCA CAG CAG CTG CTT CTC AGC-3' reverse primers. Val³⁷⁵ substitution to alanine in STIM1-ΔK construct was performed by SDM using 5'-GCT GAG AAG CAG CTG CTG GCG GCC AAG GAG GGG GCT GAG-3' forward and 5'-CTC AGC CCC CTC CTT GGC CGC CAG CAG CTG CTT CTC AGC-3' reverse primers.

All of the oligonucleotides were synthesized by Microsynth AG (Balgach). The SDM reactions were performed using Pfu Turbo DNA polymerase (Agilent Technologies). The correct clones were verified by Sanger sequencing (Microsynth AG).

Protein purification

The 6X-His-GFP tagged bacterial expression constructs were transformed into E. coli BL21 (DE3) Codon Plus strain. For pre-culture, a single colony was inoculated in 50 ml of LB containing 100 μg/ml ampicillin and cultured at 37°C for 6-8 h. The culture was then diluted to 0.1 OD₆₀₀ in 500 ml LB containing 100 μg/ml ampicillin and grown for another 1-1.5 h at 37°C until the OD₆₀₀ reached 0.4-0.6. The culture was cooled down to room temperature by incubating for 30 min. IPTG (Applchem) was added to the culture to

a final concentration of 0.25 mM to induce protein expression and the culture was grown overnight at 25°C. Next day, the culture was centrifuged at 4000 rpm for 10 min and the pellet was resuspended in 30 ml of ice-cold lysis buffer containing 50 mM Tris-HCl (pH 7.5), 250 mM NaCl, 20 mM imidazole and 0.5 mM EDTA with freshly added 1 mM PMSF, 10 mM β-mercaptoethanol and 1X Complete™ protease inhibitor cocktail (Roche). The resuspended bacteria were lysed using a microfluidizer (EmulsiFlex C5, Avestin) at a pressure of 15,000-20,000 psi. The lysate was then subjected to ultracentrifugation using a pre-cooled 45 Ti rotor at 120000 g for 45 min at 4°C. The supernatant was applied to 2 ml Ni-NTA agarose resin (Qiagen) pre-equilibrated with lysis buffer and incubated on a rotor for 1 h at 4°C. 3-5 washes with 25 ml lysis buffer were performed to eliminate non-specific binding of other proteins. Thereafter, the beads were incubated on the rotor with 2 ml elution buffer containing 50 mM Tris-HCl (pH 7.5), 250 mM NaCl and 300 mM imidazole for 1 h at 4°C. The supernatant from the beads was then loaded into dialysis membrane (Spectrum) with a molecular weight cut-off of 12-14 kDa. A step-wise dialysis was performed at 4°C for the first hour in 500 ml of 50 mM Tris-HCl (pH 7.5), 250 mM NaCl and 150 mM imidazole and for the second hour in 500 ml of 50 mM Tris-HCl (pH 7.5), 250 mM NaCl and 75 mM imidazole. Finally, overnight dialysis was performed in 1 liter of 50 mM Tris-HCl (pH 7.5) buffer containing 250 mM NaCl and no imidazole. Next day, the dialyzed proteins were collected into 1.5 ml Eppendorf tubes and stored at -20°C.

Ca²⁺/calmodulin binding assay

30 μl of the CaM affinity resin (Agilent Technologies) was washed with CaM binding buffer (25 mM Tris-HCl pH 7.5, 150 mM NaCl, 0.1% NP-40, 1 mM CaCl₂). The 6X-His-GFP recombinant proteins (1 μM) were incubated with CaM affinity resin in 600 μl of CaM binding buffer for 1 h at 4°C, rotating. The resin was then washed four times with the CaM binding buffer for elimination of any nonspecifically bound proteins. After removal of the unbound supernatant, 2X Laemmli sample buffer was added to the resin and boiled at 95°C for 5 min. Samples from the input, unbound and eluted fractions (bound) were analyzed on a 10% SDS-PAGE followed by Western blotting with a GFP antibody (SantaCruz).

CRISPR/Cas9

The Benchling CRISPR webtool (<https://benchling.com/crispr>) was used to design two different guide RNA pairs within exon 1 of human STIM1 gene. STIM1 gRNA1 (for: 5'-CAC CGT TCT GTG CCC GCG GAG ACT C-3' and rev: 5'-AAA CGA GTC TCC GCG GGC ACA GAA C-3') and gRNA2 (for: 5'-CAC CGT ATG CGT CCG TCT TGC CCT G-3' and rev: 5'-AAA CCA GGG CAA GAC GGA CGC ATA C-3') were synthesized by Microsynth AG (Balgach). These complementary gRNA oligo pairs with BbsI compatible overhangs were annealed by incubating for 5 min at 95°C in a thermocycler and then ramping down to 25°C at 5°C/min. The resulting double stranded DNA guide inserts were cloned into BbsI-digested px330.pgkpuro CRISPR/Cas9 vector [63] using T4 DNA ligase (NEB).

HEK293 cells stably overexpressing Orai1 (HEK01) seeded in a T25 flask upon reaching 70-80% confluence, were co-transfected with 2 μg of each CRISPR construct (gRNA1 and gRNA2) along with 1 μg of pmCherry-N1 using Lipofectamine® 2000 (11668019, Thermo Fisher Scientific). The mCherry-positive transfectants were sorted as single cells in a 96-well plate by FACS on BD FACSAria™ III sorter. Ten single-cell derived HEK01 cell clones were analyzed for STIM1 knock-out using a 96-well plate SOCE functional assay on Fluorometric Imaging Plate Reader (FLIPR Tetra®, Molecular Devices). A single-cell derived clone C8 was functionally confirmed to have undergone knockout of STIM1. The knock-out of STIM1 was further confirmed by Western blotting.

SOCE assay on FLIPR

HEK01 as well as HEK01 STIM1^{-/-} cell cultures were maintained at 37°C and 5% CO₂ in MEM (31095-029, Thermo Fisher Scientific) supplemented with 10% FBS (10270106, Fisher Scientific), 1% Pen/Strep (P4333, Sigma-Aldrich) and 1 μg/ml puromycin. HEK01 and HEK01 STIM1^{-/-} cells were seeded at a density of 50,000 cells/well on Corning® 96-well black polystyrene clear bottom microplates (CLS3603, Sigma-Aldrich) in 100 μl phenol red free MEM (51200-046, Thermo Fisher Scientific) supplemented with 2 mM L-Glutamine (G7513, Sigma-Aldrich). The cells were allowed to grow at 37°C and 5% CO₂ until 90-100% confluent (16-20 h).

Calcium 5 dye stock solution was prepared by dissolving a vial from Calcium 5 assay bulk kit (R8186, Molecular Devices) in 10 ml sterile-filtered nominal Ca²⁺-free (NCF), modified Krebs buffer containing 117 mM NaCl, 4.8 mM KCl, 1 mM MgCl₂, 5 mM D-glucose, 10 mM HEPES (pH 7.4) and 500 µl aliquots were stored at -20°C. The dye stock was diluted 1:20 in NCF Krebs buffer and after removing the medium of the cells, 50 µl of the diluted dye was applied per well. The cells were incubated at 37°C for 1 h in dark. The fluorescence Ca²⁺ measurements were carried out using FLIPR Tetra® where cells were excited using a 470–495 nm LED module, and the emitted fluorescence signal was filtered with a 515–575 nm emission filter (manufacturer's guidelines). Stable baselines were established for 50 sec before 50 µl of 2 µM (2X) thapsigargin (T9033, Sigma-Aldrich) freshly prepared in NCF Krebs buffer was robotically administered to the cells to deplete the Ca²⁺ stores. Cells were incubated and fluorescence was monitored in the presence of thapsigargin for a total of 10–15 min. Finally, 50 µl of 3X CaCl₂ (6 mM) prepared in NCF Krebs buffer was administered per well leading to a final 2 mM CaCl₂ concentration. The SOCE signal was recorded for another 5 min.

For transfection HEK01 STIM1^{-/-} cells were seeded at a density of 26,000 cells/well. Next day, at around 80% confluence, the cells were transfected with 100 ng/well of desired STIM1 or control plasmid DNA using Lipofectamine® 2000 (Thermo Fisher Scientific). 16–20 h post transfection, the cells were subjected to SOCE assay on FLIPR as described above.

Electrophysiology

Whole-cell patch-clamp experiments were performed as described previously [64]. Briefly, HEK01 STIM1^{-/-} cells were trypsinized and seeded into the 6-well plate. Next, when the cells reached confluence of approx. 80%, they were transiently transfected with plasmids encoding selected STIM1 mutants. Briefly, 5 µl Lipofectamine® 2000 (Thermo Fisher Scientific) and 2 µg STIM1 plasmid DNA were mixed in Opti-MEM™ (11058021, Thermo Fisher Scientific) and applied onto the cells in a single well. After 6 h of incubation with the Lipofectamine DNA complexes, cells were trypsinized and reseeded sparsely into the 35 x 10 mm (diameter x height) cell culture petri dishes.

CRAC currents were measured after 18 h of further incubation at 37 °C in humidified 5% CO₂ atmosphere. Only cells showing comparable (modest) fluorescence levels of mCherry-STIM1 were selected for recordings. The experiments were performed at room temperature, in whole-cell configuration. Pipettes were pulled from 1.5 mm thin-wall borosilicate glass capillaries with filament (BF150-86-7.5, Sutter Instruments) using a horizontal P-1000 puller (Sutter Instruments) to obtain a serial resistance of around 2.5 MΩ. Currents were recorded with PatchMaster software (HEKA Elektronik), using an EPC-10 USB amplifier (HEKA Elektronik). Upon establishment of giga seal and successful break-in into the single, mCherry fluorescent cell, 50-ms voltage ramps spanning –150 to +150 mV were delivered from a holding potential of 0 mV every 2 seconds. Currents were filtered at 2.9 kHz and digitized. Liquid junction potential was 10 mV and currents were determined and corrected before each voltage ramp. Leak currents were corrected by subtracting the initial ramp currents from all subsequent currents using FitMaster software (HEKA Elektronik). Currents were extracted at –80 and +80 mV and normalized to cell capacity (size).

Bath solution contained 120 mM NaCl, 10 mM tetraethylammonium chloride (TEA-Cl), 2 mM MgCl₂, 10 mM CaCl₂, 10 mM HEPES, and 32 mM glucose (pH 7.2 with NaOH, 300 mOsmol). Calcium-free internal solution contained 120 mM Cs-glutamate, 3 mM MgCl₂, 10 mM HEPES, 0.05 mM D-myo-inositol 1, 4,5-trisphosphate, trisodium salt (IP₃) (407137, Calbiochem), 20 mM EGTA (pH 7.2 with CsOH, 310 mOsmol with glucose). Where applicable, in order to clamp the concentration of free calcium ions at 25 nM, 2.39 mM of CaCl₂ was added to the internal solution (mentioned above) at room temperature, as calculated with the WEBMAXC standard tool available at University of California Davis Medical Center (<https://somapp.ucdmc.ucdavis.edu/pharmacology/bers/maxchelator/webmaxc/webmaxcS.htm>). When indicated, 50 µM CaM (BML-SE325-0001, Enzo Life Sciences) was added to the internal solution.

Western blotting

After running the input, unbound and eluted (bound) fractions from the CaM binding experiments on 10% SDS-PAGE, proteins were transferred onto Whatman® Protran® nitrocellulose membranes (0.45 µm pore size) by semi-dry blotting. The membranes were blocked in 5 % dry skimmed milk dissolved in 1X PBS containing 0.05 % (w/v) Tween (PBS-T) for 30 minutes at room temperature. The blots were incubated at 4 °C overnight with the rabbit polyclonal GFP antibody (sc-8334, Santa Cruz) in 1:5,000 dilution prepared in 5% milk in PBS-T. Next day the blots were washed for 20 min thrice with 1X PBS-T and incubated for 1 h

at room temperature with the anti-rabbit secondary antibody coupled to horseradish peroxidase (HRP) prepared in 5% skimmed milk in PBS-T. The blots were washed three times (20 min each) with PBS-T and finally with PBS. After incubation with the chemiluminescence blotting substrate (Roche), light emission was acquired using LAS-4000 image analyzer (Fujifilm) and ImageQuant LAS 4000 (GE Healthcare).

HEKO1 and HEKO1 STIM1^{-/-} cells after washing with PBS were lysed using ice-cold RIPA buffer (150 mM NaCl, 50 mM Tris-HCl pH 7.4, 5 mM EDTA, 1% Triton-X-100, 0.5% Deoxycholate, 0.1% SDS) with freshly added 1X protease inhibitor cocktail (Roche). Total cell lysates were spun down at 15,000 g for 10 min at 4°C. The supernatants were collected, and protein estimation was performed using DC™ protein assay (Bio-Rad). 20 µl cell lysate for each sample containing 20 µg total protein and 1X Laemmli buffer was separated on 10% SDS-PAGE. Similar procedure as described above was followed for Western blotting. Mouse monoclonal hOrai1 antibody (SAB4200273, Sigma-Aldrich) was used in a 1:200 dilution. Mouse monoclonal Tubulin antibody (T9028, Sigma-Aldrich) was used in a 1:2,000 dilution. Guinea pig polyclonal hSTIM1 antibody [62] raised against the N-terminus of hSTIM1 (residues 23-213) was used in a 1:1,000 dilution. HRP conjugated goat anti-mouse secondary antibody was used in a 1:3,000 dilution (172-1011, Bio-Rad). Peroxidase-conjugated affinity-pure goat anti-guinea pig secondary antibody was used in a 1:10,000 dilution (106-035-003, Jackson Immuno Research). The antibodies were prepared as above. After incubation of the membranes with the Western blotting substrate (RPN2106, GE Healthcare), the chemiluminescence was detected on an Amersham™ Hyperfilm™ MP (GE Healthcare).

Analysis software and statistics

ImageJ was used to quantify the density of the bands from the Western blots of the CaM binding experiments. Fluorescence signals from FLIPR Tetra® were analyzed using the ScreenWorks 3.1.1.8 software (Molecular Devices). The SOCE activity was measured by quantifying the area under the curve (AUC) and slope of the curve of the fluorescence intensity trace(s), following administration of the final 2 mM CaCl₂. The data are plotted as mean ± S.D. Igor Pro 6.3.7.2 (WaveMetrics) was used for I_{CRAC} data analysis and the data are plotted as mean ± S.E.M. The statistical evaluation was carried out using both Student's t- and Mann Whitney U non-parametric tests using Microsoft® Excel and IBM® SPSS® v20.

Results

Critical residues for calmodulin binding within the SOAR domain

Ca²⁺/CaM is known to bind targets with two hydrophobic anchor residues spaced eight, twelve or fourteen residues apart from each other [65-68]. Our in silico analysis of the STIM1 sequence on the CaM-target database server [69] revealed a putative CaM binding site within the evolutionary conserved SOAR domain of STIM1. We identified two hydrophobic sites (H1 and H2) that may serve as anchors for Ca²⁺/CaM binding (Fig. 1A).

To investigate the role of hydrophobic interactions in STIM1-Ca²⁺/CaM complex formation exclusive of the Ca²⁺/CaM binding K-rich domain, we used recombinant protein constructs encoding N-terminally hexa-histidine and GFP-tagged STIM1 cytosolic terminus lacking the K-rich domain (STIM1CT-ΔK). We mutated the following residues from H1 or H2 to alanines: Leu³⁷⁴ and Val³⁷⁵ from H1 (H1AA) and Leu³⁹⁰ and Phe³⁹¹ from H2 (H2AA), or both in combination (H1AA-H2AA) and assessed protein binding to Ca²⁺/CaM-sepharose beads (Fig. 1B and C). The H2AA mutation led to approximately a 75% decrease in protein binding to Ca²⁺/CaM confirming previous findings of Li et al. with respect to the involvement of these residues of STIM1 in Ca²⁺/CaM binding (Fig. 1B). The mutation of our newly identified H1 site (H1AA) led to a 66% decrease in protein binding to Ca²⁺/CaM. These findings uncover that residues from both sites, H1 and H2, serve as hydrophobic anchors for Ca²⁺/CaM binding (Fig. 1B). The combined mutation of these hydrophobic residues at sites H1 and H2 (H1AA-H2AA) did not result in any further decrease in protein binding (Fig. 1C). Deletion of the entire CaMBD_{SOAR} domain from STIM1CT-ΔK led to a 90% drop in Ca²⁺/CaM binding (Fig. 1C). Overall, these findings highlight the significance of the hydrophobic residues at H1 and H2 sites in CaMBD_{SOAR} for the formation of a STIM1-Ca²⁺/CaM complex.

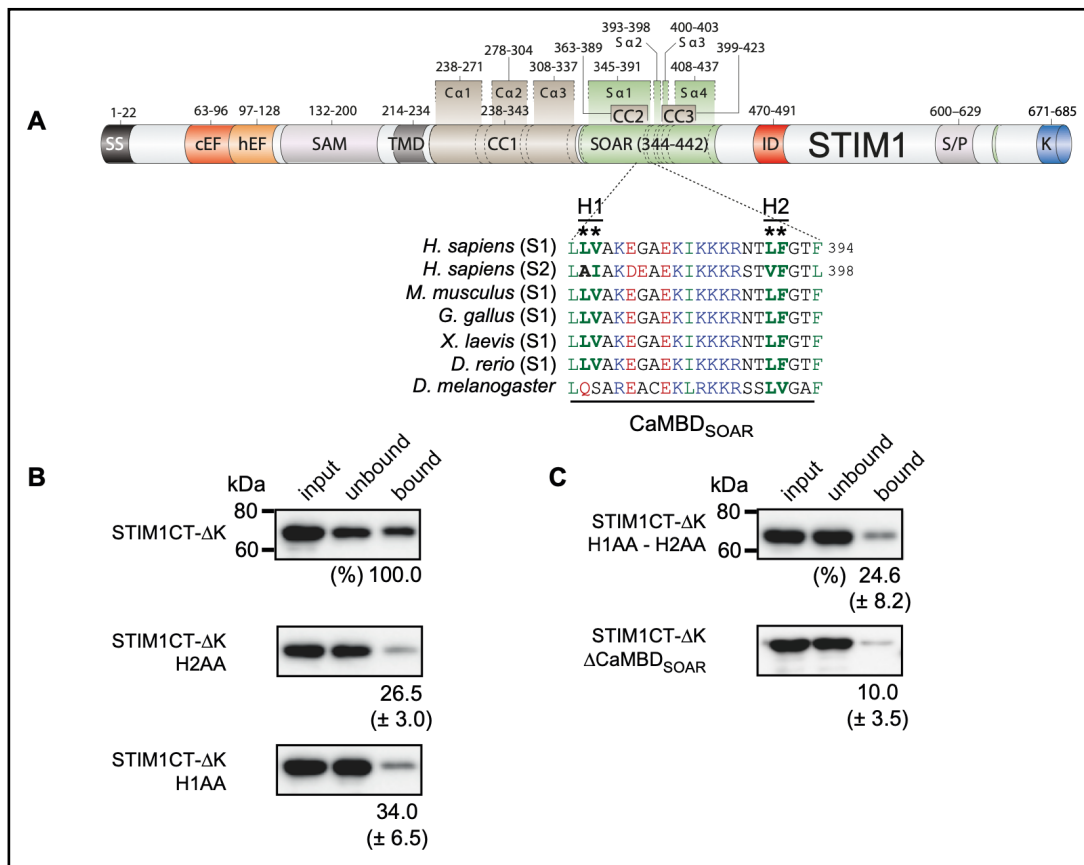
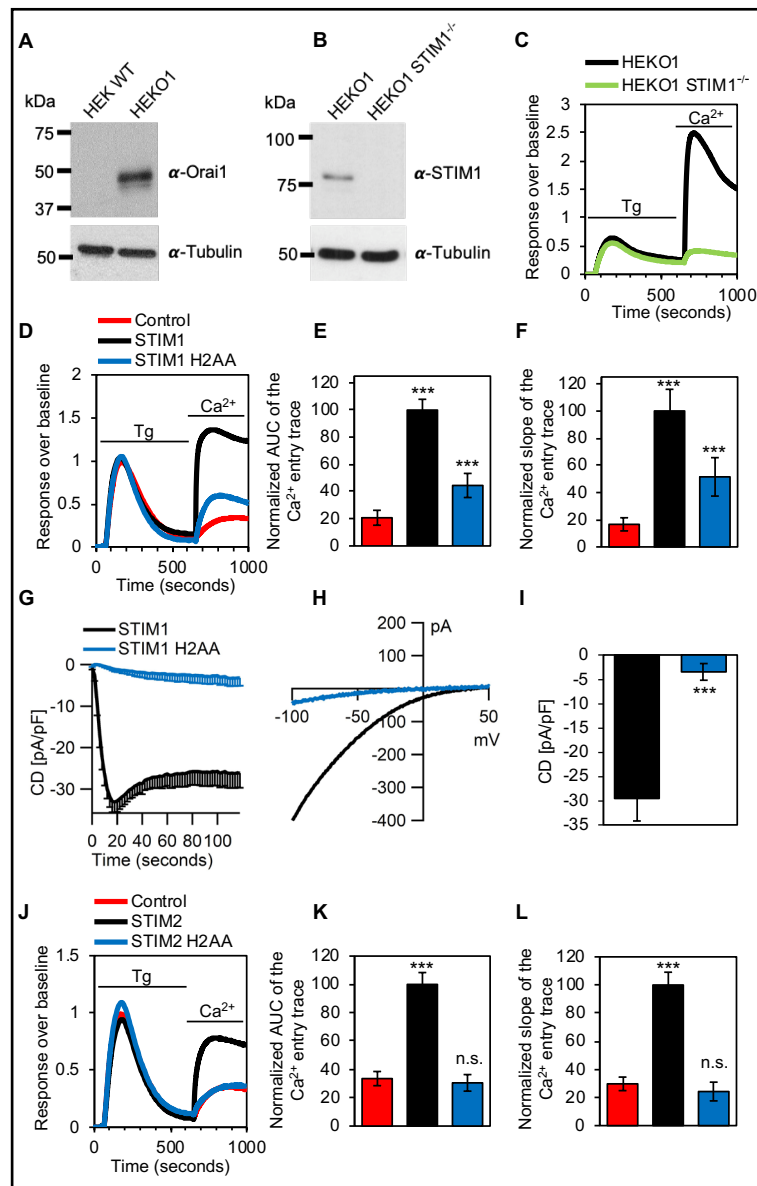


Fig. 1. Hydrophobic residues crucial for binding of Ca²⁺/Calmodulin to STIM1-Orai1 activating region. (A), Domain architecture of human STIM1 with sequence alignment of predicted CaM-binding domains (CaMBDs) of human STIM1 and STIM2 and STIM1 of different vertebrates and drosophila are shown. Conserved hydrophobic residues (H1 and H2) in STIM1-Orai1 activating region (SOAR) are indicated in bold green within CaMBD_{SOAR} (residues 372-394) and are marked with asterisks. (B), Binding of GFP-tagged STIM1 C-terminus lacking the K-rich domain (STIM1CT-ΔK) and STIM1CT-ΔK with mutations of hydrophobic residues (L390A-F391A = H2AA and L374A-V375A = H1AA) in CaMBD_{SOAR} to CaM beads. C, Binding of STIM1CT-ΔK with combined H2AA and H1AA mutations and of STIM1CT-ΔK with deletion of CaMBD_{SOAR} to CaM beads. The bound fraction of STIM1CT-ΔK was set to 100 in all three experiments and the mean ± S.E.M. for the bound (eluted) fractions of all mutants is indicated.

The H2 site of STIM1 CaMBD_{SOAR} is critical for Orai1 activation

For further investigations, we generated a STIM1 deficient HEK293 cell line to eliminate endogenous STIM1 background expression. We knocked out STIM1 (STIM1^{-/-}) in HEK293 cells stably overexpressing human wild type Orai1 (HEKO1) [70] using the CRISPR/Cas9 technique. Orai1 and STIM1 protein levels in HEKO1 cells and HEKO1 STIM1^{-/-} cells are shown by Western blot analysis (Fig. 2A and B). Knockout of STIM1 in HEKO1 cells nearly abolished SOCE (Fig. 2C). Conversely, overexpression of human wildtype STIM1 in HEKO1 STIM1^{-/-} cells rescued SOCE compared to control transfected cells (Fig. 2D). A thorough analysis of SOCE (area under the curve and rate of Ca²⁺ entry) is shown (Fig. 2E and F). Only a minor but significant rescuing effect was observed in cells expressing STIM1 H2AA (Fig. 2D, E and F). Next, I_{CRAC} was evoked with 20 mM EGTA and 50 μM IP₃ in the patch pipette. Consistent with the SOCE findings, expression of STIM1 H2AA in HEKO1 STIM1^{-/-} cells resulted in significantly smaller I_{CRAC} compared to STIM1 WT (Fig. 2G, H and I). The substitution of both H2 residues by serine (H2SS) completely failed to rescue SOCE and I_{CRAC} (Supplementary Fig. S1 – for all

Fig. 2. H2 site mutants of STIM1 CaM-binding domain show impaired Orai1 activation in HEK293 cells. (A), Anti-Orai1 Western blot of HEK293 wild type and HEK293 cells stably overexpressing Orai1 (HEK01). (B), Anti-STIM1 Western blot of HEK01 and STIM1 knock-out HEK01 (HEK01 STIM1^{-/-}) cells. (C), Representative FLIPR traces of calcium entry after thapsigargin mediated store-depletion in HEK01 (black) and HEK01 STIM1^{-/-} (green) cells. 1 μM thapsigargin (Tg) and 2 mM CaCl₂ (Ca²⁺) administrations are indicated. (D), Representative FLIPR traces of SOCE in HEK01 STIM1^{-/-} cells transiently transfected with mCherry (Control, red), mCherry-STIM1 (STIM1, black) or mCherry-STIM1-L390A-F391A (STIM1 H2AA, blue). (E), Quantified area under the curve (AUC) and (F), slope of the SOCE traces after extracellular Ca²⁺ application in HEK01 STIM1^{-/-} cells transiently transfected with control (red), STIM1 (black) or STIM1 H2AA (blue). The data was normalized by setting the AUC and slope of the Ca²⁺ entry traces to 100 (n = 15; mean ± standard deviation). (G), average current density (CD) of the I_{CRAC} recordings (STIM1, n = 9; STIM1 H2AA, n = 6; mean - SEM) from HEK01 STIM1^{-/-} cells. (H), average current-voltage (I-V) curves of the I_{CRAC} recordings at t = 2 min (STIM1, n = 9; STIM1 H2AA, n = 6). (I), quantified average CD values at t = 2 min (STIM1, n = 9; STIM1 H2AA, n = 6; mean ± SEM) from HEK01 STIM1^{-/-} cells transiently overexpressing STIM1 (black) or STIM1 H2AA (blue). (J), Representative FLIPR traces of SOCE in HEK01 STIM1^{-/-} cells transiently transfected with mCherry (Control, red), mCherry-STIM2 (STIM2, black) or mCherry-STIM2-V394A-F395A (STIM2 H2AA, blue). (K), Quantified AUC and (L), slope of the SOCE traces after extracellular Ca²⁺ application in HEK01 STIM1^{-/-} cells transiently overexpressing control (red), STIM2 (black) or STIM2 H2AA (blue). The data was normalized by setting the AUC and slope of the Ca²⁺ entry traces to 100 (n = 15; mean ± standard deviation). p value (p) of the WT or mutant STIM compared to the mcherry control group is indicated above the respective bar as non-significant (n.s.) for p > 0.05 or as “***” for p <= 0.001.



supplemental material see www.cellphysiolbiochem.com) consistent with earlier findings [61]. In addition, we tested whether corresponding H2 residues in STIM2 are involved in Orai1 activation. Given the alignment of STIM1 and STIM2 (Fig. 1A), residues Leu³⁹⁰ and Phe³⁹¹ in STIM1 correspond to residues Val³⁹⁴ and Phe³⁹⁵ in STIM2. Overexpression of human wildtype STIM2 in HEK01 STIM1^{-/-} cells resulted in an increase of SOCE compared to control transfected cells (Fig. 2J, K and L). Expression of STIM2 V394A-F395A (STIM2 H2AA) did not increase SOCE above control levels (Fig. 2J, K and L). Taken together, our results indicate that either, or both hydrophobic residues in STIM1 and STIM2 CaMBD_{SOAR} H2 site are important for activation of SOCE.

Phe³⁹¹ within H2 of the STIM1 CaMBD_{SOAR} is linked to Orai1 activation

Several residues within, or close to the STIM1 H1 and H2 sites of the CaMBD_{SOAR} (Phe³⁹⁴, Leu³⁹⁰, Ile³⁸³, Ala³⁷⁶ and Leu³⁷³) are crucial for Orai1 coupling and activation [71-74]. In addition, several basic residues spanning CaMBD_{SOAR} (Lys³⁸⁴, Lys³⁸⁵ and Lys³⁸⁶) are required for Orai1 activation [75-77]. Thus, it is difficult to evaluate whether contributions of individual residues of the H2 site of STIM1 are related to Ca²⁺/CaM-mediated SCDI, as the observed effects may simply be a result of altered Orai1 activation. Recently, the L390A substitution in STIM1 was shown to significantly impair Orai1 activation, abolishing I_{CRAC} [74]. Therefore, we focused on substitutions of F391 in STIM1-ΔK. We mutagenized F391 to amino acids with less hydrophobic side chains (valine or alanine) or to amino acids characterized by side chain hydrophobicity in the same range as phenylalanine (i.e. tryptophan or leucine) [78]. When compared to STIM1-ΔK in HEK01 STIM1^{-/-} cells, expression of STIM1-ΔK F391A or STIM1-ΔK F391V resulted in reduced SOCE (Fig. 3A, B and C). Upon expression of STIM1-ΔK F391L, SOCE remained unchanged and upon expression of STIM1-ΔK F391W, a slight increase in SOCE was observed, compared to STIM1-ΔK (Fig. 3A, B and C). When analyzing the effects of the F391 mutants on I_{CRAC}, only the substitution of STIM1-ΔK F391W preserved similar I_{CRAC} compared to STIM1-ΔK (Fig. 3D, E and F). Substitutions of F391 with either valine or leucine resulted in a ~2-fold lower current density compared to STIM1-ΔK (Fig. 3D, E and F). When STIM1-ΔK F391A was expressed, I_{CRAC} was reduced by ~85% (Fig. 3D, E and F). Strikingly, less hydrophobic substitutions of STIM1 F391 that are expected to mediate weaker Ca²⁺/CaM binding resulted in reduced SOCE instead of an increase in SOCE, under conditions that favor SCDI (Fig. 3A, B and C). In patch clamp experiments designed to prevent SCDI, several mutants of F391 resulted in reduced I_{CRAC} per se (Fig. 3D, E and F). As shown before in Fig. 2, these results indicate that mutations in the H2 site of STIM1 directly alter Orai1 activity, independently of Ca²⁺/CaM-mediated SCDI. For this reason, STIM1 H2 mutants were not further analyzed in context of STIM1-dependent, Ca²⁺/CaM-mediated SCDI of I_{CRAC}.

Contrary to H2, the H1 residues of CaMBD_{SOAR} are not linked to Orai1 activation

We next assessed the effect of alanine substitutions at the H1 site of CaMBD_{SOAR} on SOCE and I_{CRAC} (see Fig. 1A). The H1AA mutant of STIM1 did not show any deficit in rescuing SOCE in HEK01 STIM1^{-/-} cells (Fig. 4A, B and C). STIM1-ΔK H1AA also mediated a comparable I_{CRAC} response with similar I-V characteristics as STIM1-ΔK (Fig. 4D, E and F).

To further pin down the role of H1 residues in SOCE regulation, we substituted the residue Val³⁷⁵ to the more hydrophobic tryptophan residue (STIM1-ΔK V375W) or the less hydrophobic alanine residue (STIM1-ΔK V375A) [78]. None of the mutations changed SOCE (Fig. 4G, H and I) or I_{CRAC}, when compared to STIM1-ΔK (Fig. 4J, K and L). In conclusion, our findings demonstrate that the STIM1 Val³⁷⁵ hydrophobic residue at the H1 site is not critical for Orai1 activation. Hence, we further investigated Val³⁷⁵ in STIM1-dependent, Ca²⁺/CaM-mediated SCDI of I_{CRAC}.

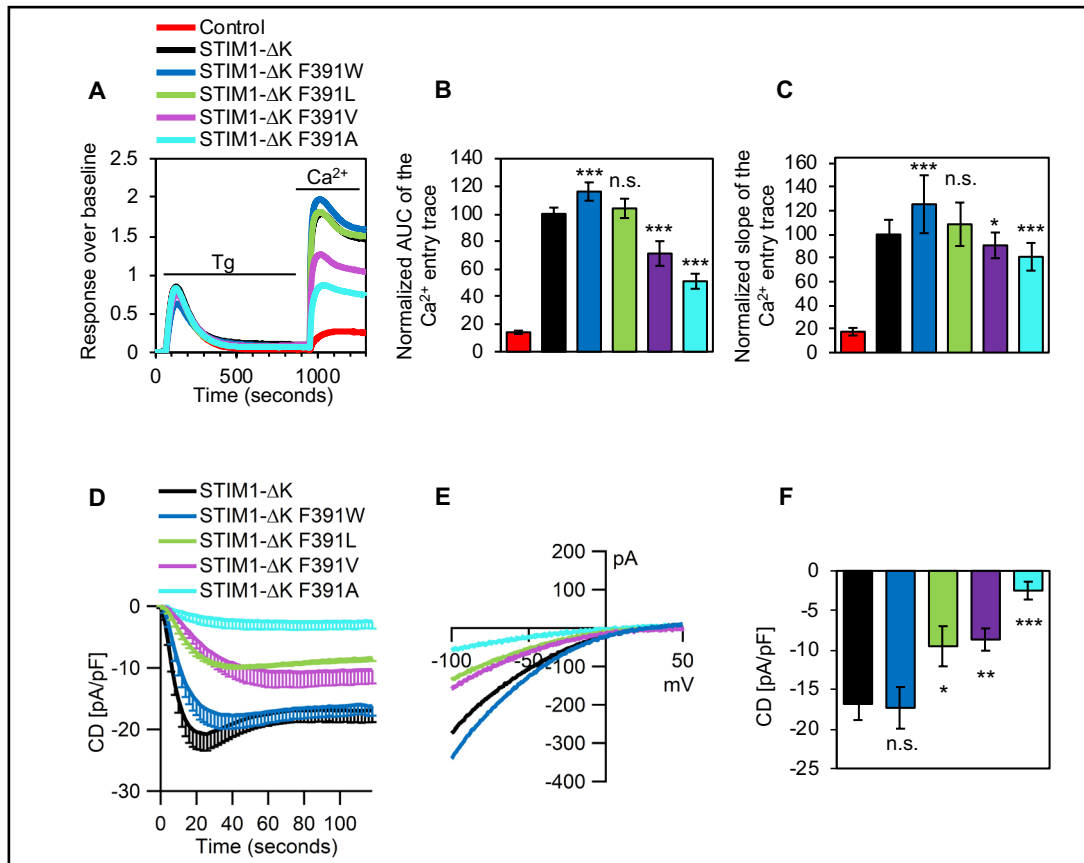
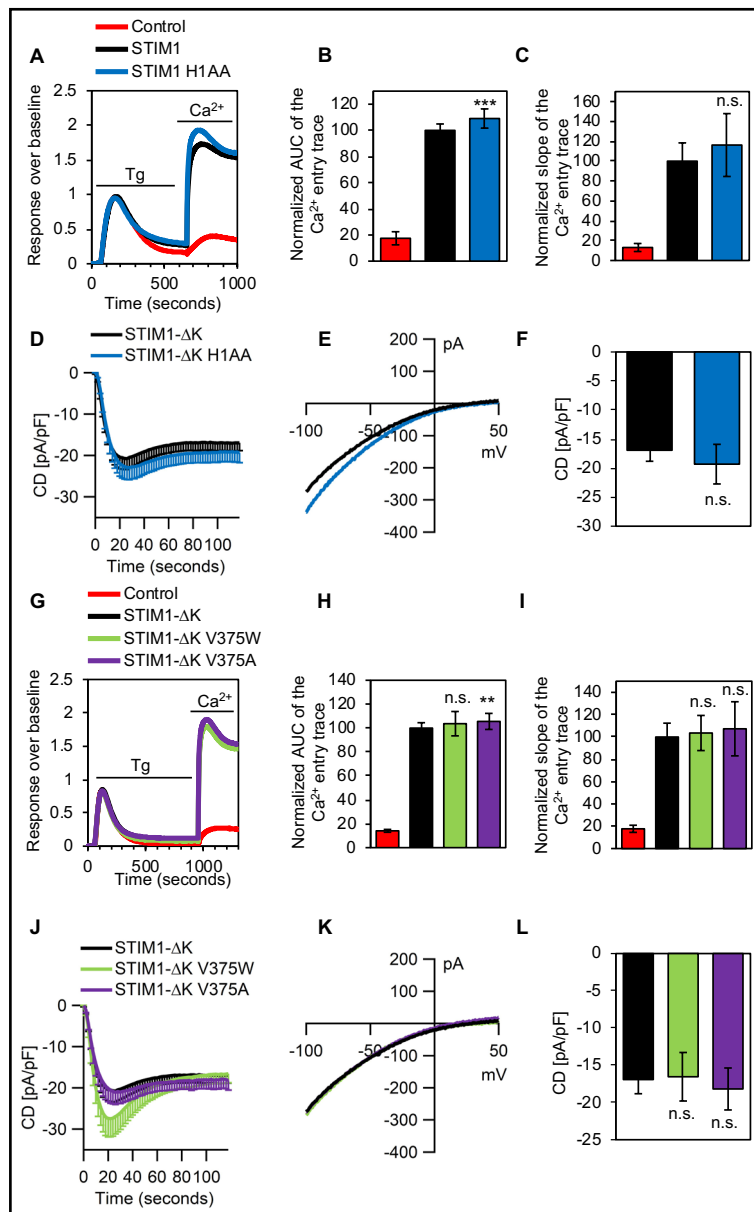


Fig. 3. Phe³⁹¹ is a critical residue for the Orai1 activation function of STIM1. (A), Representative FLIPR traces of SOCE in HEK01 STIM1^{-/-} cells transiently transfected with mCherry (Control, red), mCherry-STIM1-ΔK (STIM1-ΔK, black), mCherry-STIM1-ΔK F391W (STIM1-ΔK F391W, blue), mCherry-STIM1-ΔK F391L (STIM1-ΔK F391L, green), mCherry-STIM1-ΔK F391V (STIM1-ΔK F391V, purple) or mCherry-STIM1-ΔK F391A (STIM1-ΔK F391A, aqua). 1 μM thapsigargin (Tg) and 2 mM CaCl₂ (Ca²⁺) administrations are indicated. (B), Quantified area under the curve (AUC) and (C), slope of the SOCE traces after extracellular Ca²⁺ application in HEK01 STIM1^{-/-} cells transiently transfected with control (red), STIM1-ΔK (black), STIM1-ΔK F391W (blue), STIM1-ΔK F391L (green), STIM1-ΔK F391V (purple) or STIM1-ΔK F391A (aqua). The data was normalized by setting the AUC and slope of the Ca²⁺ entry traces to 100 (n = 18; mean ± standard deviation). (D), average current density (CD) of the I_{CRAC} recordings (STIM1-ΔK, n = 14; STIM1-ΔK F391W, n = 8; STIM1-ΔK F391L, n = 5; STIM1-ΔK F391V, n = 6; STIM1-ΔK F391A, n = 4; mean - SEM) from HEK01 STIM1^{-/-} cells. (E), average current-voltage (I-V) curves of the I_{CRAC} recordings at t = 2 min from the traces shown in D. (F), quantified average CD values at t = 2 min (STIM1-ΔK, n = 14; STIM1-ΔK F391W, n = 8; STIM1-ΔK F391L, n = 5; STIM1-ΔK F391V, n = 6; STIM1-ΔK F391A, n = 4; mean ± SEM) from HEK01 STIM1^{-/-} cells transiently overexpressing STIM1-ΔK (black), STIM1-ΔK F391W (blue), STIM1-ΔK F391L (green), STIM1-ΔK F391V (purple) or STIM1-ΔK F391A (aqua). p value (p) of each of the STIM1-ΔK Phe³⁹¹ mutant compared to the STIM1-ΔK group is indicated above the respective bar as non-significant (n.s.) for p > 0.05, "*" for p ≤ 0.05, "***" for p ≤ 0.01 or "****" for p ≤ 0.001.

Fig. 4. The H1 site residues of STIM1 CaM-binding domain are dispensable for Orai1-activating function of STIM1. (A), Representative FLIPR traces of SOCE in HEK01 STIM1^{-/-} cells transiently transfected with mCherry (Control, red), mCherry-STIM1 (STIM1, black) or mCherry-STIM1-L374A-V375A (STIM1 H1AA, blue). 1 μM thapsigargin (Tg) and 2 mM CaCl₂ (Ca²⁺) administrations are indicated. (B), Quantified area under the curve (AUC) and (C), slope of the SOCE traces after extracellular Ca²⁺ application in HEK01 STIM1^{-/-} cells transiently transfected with control (red), STIM1 (black) or STIM1 H1AA (blue). The data was normalized by setting the AUC and slope of the Ca²⁺ entry traces to 100 (n = 15; mean ± standard deviation). (D), average current density (CD) of the I_{CRAC} recordings (STIM1-ΔK, n = 15; STIM1-ΔK H1AA, n = 7; mean - SEM) from HEK01 STIM1^{-/-} cells. (E), average current-voltage (I-V) curves of the I_{CRAC} recordings at t = 2 min from the traces shown in D. (F), quantified average CD values at t = 2 min (STIM1-ΔK, n = 15; STIM1-ΔK H1AA, n = 7; mean ± SEM) from HEK01 STIM1^{-/-} cells transiently overexpressing STIM1-ΔK (black) or STIM1-ΔK H1AA (blue). p value (p) of the STIM1- or STIM1-ΔK H1AA mutant compared to the STIM1 or STIM1-ΔK group, respectively is indicated above the respective bar as non-significant (n.s.) for p > 0.05 or “***” for p ≤ 0.001. (G), Representative FLIPR traces of SOCE in HEK01 STIM1^{-/-} cells transiently transfected with control (red), STIM1-ΔK (black), STIM1-ΔK V375W (green) or STIM1-ΔK V375A (purple). (H), Quantified area under the curve (AUC) and (I), slope of the SOCE traces after extracellular Ca²⁺ application shown in G. The data was normalized by setting the AUC and slope of the Ca²⁺ entry traces to 100 (n = 18; mean ± standard deviation). (J), average current density (CD) of the I_{CRAC} recordings (STIM1-ΔK, n = 15; STIM1-ΔK V375W, n = 6; STIM1-ΔK V375A, n = 10; mean - SEM) from HEK01 STIM1^{-/-} cells. (K), average I-V curves of the I_{CRAC} recordings at t = 2 min from the traces shown in J. (L), quantified average CD values at t = 2 min (STIM1-ΔK, n = 15; STIM1-ΔK V375W, n = 6; STIM1-ΔK V375A, n = 10; mean ± SEM) from HEK01 STIM1^{-/-} cells transiently overexpressing STIM1-ΔK (black), STIM1-ΔK V375W (green) or STIM1-ΔK V375A (purple). p value (p) of each of the STIM1-ΔK Val³⁷⁵ mutant compared to the STIM1-ΔK group is indicated above the respective bar as non-significant (n.s.) for p > 0.05 or “***” for p ≤ 0.01.

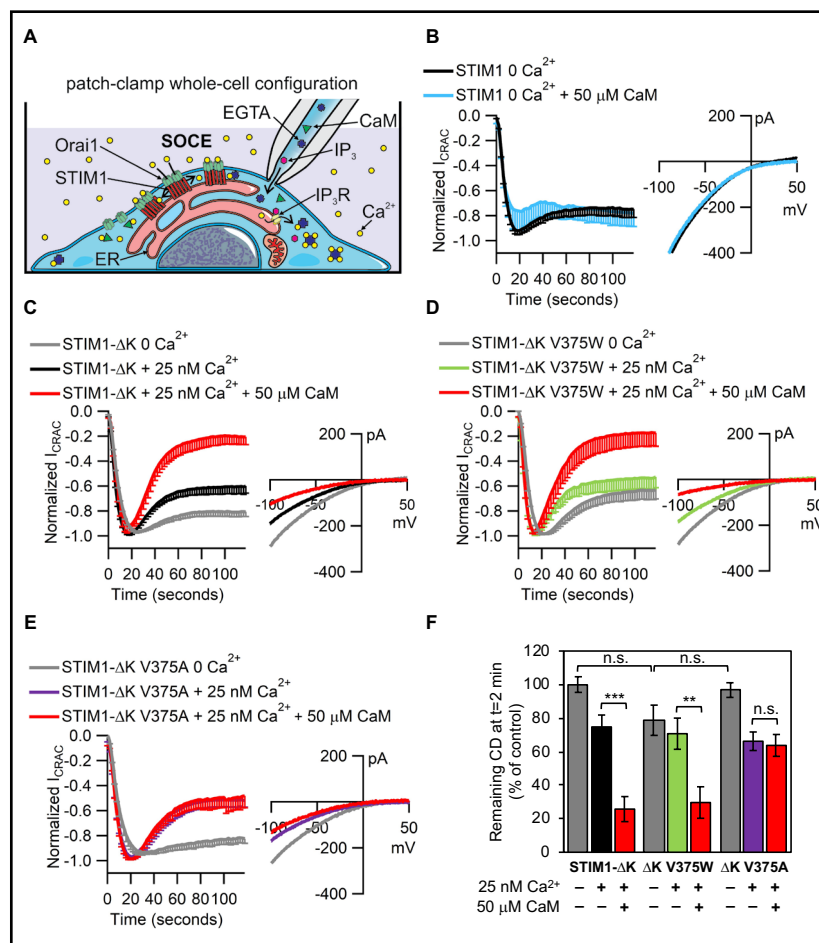


STIM1 Val³⁷⁵ is critical for Ca²⁺/CaM-mediated SCDI of I_{CRAC}

To examine Ca²⁺/CaM-mediated SCDI, we first investigated whether CaM alone in absence of intracellular calcium ([Ca²⁺]_i) affects SCDI of STIM1/Orai1-mediated I_{CRAC}. Fig. 5A illustrates the whole-cell patch-clamp procedure designed and implemented to address this question. When [Ca²⁺]_i was clamped to near zero with 20 mM EGTA, we observed no effect of 50 μM CaM on SCDI of I_{CRAC} (Fig. 5B). In the presence of 25 nM [Ca²⁺]_i and 50 μM CaM, STIM1-ΔK/Orai1-mediated I_{CRAC} decayed by ~75% in 2 min after break in, but only decayed by ~25% when only 25 nM [Ca²⁺]_i was present (Fig. 5C and F). This suggests a role for cytosolic Ca²⁺/CaM in SCDI of I_{CRAC}.

We observed that STIM1-ΔK V375W/Orai1-mediated I_{CRAC} had preserved SCDI compared to STIM1-ΔK and underwent ~60% decay in the presence of both 25 nM [Ca²⁺]_i and 50 μM CaM, compared to only ~10% decay in the presence of 25 nM [Ca²⁺]_i alone (Fig. 5D and F).

Fig. 5. Val³⁷⁵ of STIM1 is a critical for Ca²⁺/CaM-mediated SCDI of I_{CRAC}. (A), Cartoon illustrating the patch-clamp electrophysiology experimental setup. (B), average normalized current density (CD) of the I_{CRAC} recordings (STIM1 0 [Ca²⁺]_i, n = 10; STIM1 0 [Ca²⁺]_i + 50 μM CaM, n = 5; mean - SEM) from HEK01 STIM1^{-/-} cells and average current-voltage (I-V) curves of the I_{CRAC} recordings at t = 2 min. (C), average normalized current density (CD) of the I_{CRAC} recordings (STIM1-ΔK + 0 [Ca²⁺]_i, n = 15; STIM1-ΔK + 25 nM [Ca²⁺]_i, n = 11; STIM1-ΔK + 25 nM [Ca²⁺]_i + 50 μM CaM, n = 8; mean - SEM) from HEK01 STIM1^{-/-} cells and average I-V curves of the I_{CRAC} recordings at t = 2 min. (D), average normalized



current density (CD) of the I_{CRAC} recordings (STIM1-ΔK V375W + 0 [Ca²⁺]_i, n = 6; STIM1-ΔK V375W + 25 nM [Ca²⁺]_i, n = 6; STIM1-ΔK V375W + 25 nM [Ca²⁺]_i + 50 μM CaM, n = 8; mean - SEM) from HEK01 STIM1^{-/-} cells and average I-V curves of the I_{CRAC} recordings at t = 2 min. (E), average normalized current density (CD) of the I_{CRAC} recordings (STIM1-ΔK V375A + 0 [Ca²⁺]_i, n = 8; STIM1-ΔK V375A + 25 nM [Ca²⁺]_i, n = 9; STIM1-ΔK V375A + 25 nM [Ca²⁺]_i + 50 μM CaM, n = 9; mean - SEM) from HEK01 STIM1^{-/-} cells and average I-V curves of the I_{CRAC} recordings at t = 2 min. (F), average of the remaining CD at t = 2 min from individual traces shown in C, D and E (mean ± SEM). The average of the remaining CD at t = 2 min of STIM1-ΔK with 0 [Ca²⁺]_i was set to 100 for normalization. Addition of either 25 nM [Ca²⁺]_i alone or together with 50 μM CaM is indicated below the bar graphs. p value (p) of each of the CaM added condition compared to its respective without CaM condition is indicated as non-significant (n.s.) for p > 0.05 or “**” for p ≤ 0.01 or “***” for p ≤ 0.001.

In contrast, addition of CaM together with 25 nM [Ca²⁺]_i did not show any enhancement in SCDI of STIM1-ΔK V375A/Orai1-mediated I_{CRAC}, compared to the current in presence of only 25 nM [Ca²⁺]_i (Fig. 5E and F).

Mutations in H1 do not alter activation of Orai1. Hydrophobic residue valine or tryptophan at 375 residue position in H1 is essential for Ca²⁺/CaM-mediated SCDI, as less hydrophobic amino acid alanine prevents SCDI. STIM1 Val³⁷⁵ in the H1 site controls Ca²⁺/CaM-mediated SCDI of I_{CRAC}. In summary, our findings provide direct evidence that binding of Ca²⁺/CaM to STIM1 at the CaMBD_{SOAR} triggers SCDI.

Discussion

For many years, activation of store-operated CRAC channels has been subject to intensive investigations. One regulatory mechanism, that prevents Ca²⁺ overload upon I_{CRAC} activation is SCDI. In our study, we examined STIM1-dependent, Ca²⁺/CaM-mediated SCDI. We identified two hydrophobic anchor sites for Ca²⁺/CaM in STIM1, H1 and H2. The latter has been described earlier in the context of Ca²⁺/CaM mediated SCDI [61]. However, the study was limited by the usage of a non-functional STIM1 H2SS construct, that does not allow for the analysis of I_{CRAC} SCDI. Consistently, in our hands, STIM1 H2SS failed to elicit SOCE or I_{CRAC} probably as STIM1 H2SS did not oligomerize, form ER-PM contact sites in response to store depletion and did not interact with Orai1 [61].

In our study, we used a well-defined HEK293 expression system, lacking endogenous STIM1, and stably overexpressing Orai1, wherein we overexpressed K-rich domain deficient STIM1 constructs. The deletion of K-rich domain of STIM1 excludes recruitment of Ca²⁺/CaM to this domain, and prevents participation of SARAF in SCDI [43].

CaM binding assays, Ca²⁺ imaging and patch clamp experiments with STIM1 H2AA demonstrate that Leu³⁹⁰/Phe³⁹¹ (H2) residues are required for both Orai1 activation and Ca²⁺/CaM binding. Single residue mutations of Phe³⁹¹ resulted in altered Orai1 activation. Hence, analysis of structure-function relationship between H2 and Ca²⁺/CaM-dependent SCDI cannot be precisely evaluated. In contrast, H1 binds Ca²⁺/CaM and mutations did not alter Orai1 activation. Mutations of both Leu³⁷⁴ and Val³⁷⁵ or Val³⁷⁵, did not change Orai1 activation but were critical for Ca²⁺/CaM-mediated SCDI of I_{CRAC}. Notably, mutation of hydrophobic Val³⁷⁵ to hydrophobic tryptophan did not alter Ca²⁺/CaM-mediated SCDI, probably since replacement by another hydrophobic residue does not change Ca²⁺/CaM binding properties. In contrast, a change to the less hydrophobic alanine completely abolished Ca²⁺/CaM-mediated SCDI.

The STIM2 SOAR domain residues 372-395 (corresponding to STIM1 368-391 residues) and the K-rich domain of STIM2 have both been shown to bind Ca²⁺/CaM [16, 55]. The Val³⁷⁵ residue position in STIM1 that we found to be critical for Ca²⁺/CaM-assisted SCDI corresponds to I379 in STIM2. Isoleucine is even more hydrophobic and bulkier than valine [78], indicating a role for I379 in STIM2 dependent Ca²⁺/CaM-mediated SCDI. In our hands, STIM2 H2AA did not activate Orai1, further highlighting a role of these residues in Orai1 activation by both STIM isoforms. Future studies will be required to show if I379 and/or the K-rich domain of STIM2 are required for Ca²⁺/CaM-mediated inactivation of STIM2/Orai1-elicited I_{CRAC} and/or constitutive currents [79].

Conclusion

We here propose a mechanistic model, wherein binding of Ca²⁺/CaM to STIM1 hydrophobic sites H1 and H2 within CaMBD_{SOAR} triggers SCDI of I_{CRAC}. We show that H1 is not critical for Orai1 activation but for Ca²⁺/CaM binding. We demonstrate that the H1 residue Val³⁷⁵ is dispensable for CRAC channel activation but crucial for Ca²⁺/CaM-mediated SCDI of I_{CRAC}. Also, H2 hydrophobic site is bifunctional: It is linked to both Orai1 activation and Ca²⁺/CaM-binding, with a likely role in mediating SCDI that cannot be segregated. Taken

together, we demonstrate that CaMBD_{SOAR} directly coordinates Ca²⁺/CaM-mediated SCDI of CRAC channels and we dissected the roles of CaMBD_{SOAR} residues in Orai1 activation and Ca²⁺/CaM-mediated SCDI. We therefore reveal a fundamental role for STIM1 in coordinating Ca²⁺/CaM dependent SCDI of CRAC channels.

Acknowledgements

We thank T. Locher and Y. Amrein for excellent technical assistance. We would like to thank Dr. Stefan Mueller and Thomas Schaffer at the FACS facility, Institute of Pathology, University of Bern for their help in FACS sorting. We also thank Profs. Ivan Bogeksi and Barbara A. Niemeyer for providing the HEK01 STIM1^{-/-} cells generated by Dr. Dalia Alansary. We are very grateful to Prof. Nicolas Demaurex for his important feedback on the manuscript.

Statement of Ethics

The authors have no ethical conflicts to disclose.

Funding Sources

This work was supported by the Sinergia SNF grants CRSII5_180326 and CRSII3_160782 to M.A.H.

Author Contributions

R.B. and C.P. designed the study, and M.A.H. and C.P. coordinated the study. R.B. and B.S.A. prepared the figures and R.B. wrote the manuscript. R.B. generated all the mammalian expression constructs and performed the FLIPR Tetra[®] Ca²⁺ imaging experiments and B.S.A. performed all the electrophysiology experiments, under the supervision of M.A.H. and C.P. E.E-H. generated the bacterial expression constructs and performed the Ca²⁺/CaM binding experiments under the supervision of M.S. during her PhD at the University of Heidelberg. R.B. and P.K. generated the HEK01 STIM1^{-/-} cells using CRISPR/Cas9 technique. All authors have read and approved the final version of this manuscript and agree to be accountable for all aspects of the work in ensuring that questions related to the accuracy or integrity of any part of the work are appropriately investigated and resolved. All persons designated as authors qualify for authorship, and all those who qualify for authorship are listed.

Disclosure Statement

The authors have no conflicts of interest to declare.

References

- 1 Prakriya M, Lewis RS: Store-Operated Calcium Channels. *Physiol Rev* 2015;95:1383-1436.
- 2 Liou J, Kim ML, Heo WD, Jones JT, Myers JW, Ferrell JE Jr, Meyer T: STIM is a Ca²⁺ sensor essential for Ca²⁺-store-depletion-triggered Ca²⁺ influx. *Curr Biol* 2005;15:1235-1241.
- 3 Roos J, DiGregorio PJ, Yeromin AV, Ohlsen K, Lioudyno M, Zhang S, Safrina O, Kozak JA, Wagner SL, Cahalan MD, Velicellebi G, Stauderman KA: STIM1, an essential and conserved component of store-operated Ca²⁺ channel function. *J Cell Biol* 2005;169:435-445.
- 4 Vig M, Peinelt C, Beck A, Koomoa DL, Rabah D, Koblan-Huberson M, Kraft S, Turner H, Fleig A, Penner R, Kinet JP: CRACM1 is a plasma membrane protein essential for store-operated Ca²⁺ entry. *Science* 2006;312:1220-1223.
- 5 Zhang SL, Yeromin AV, Zhang XH, Yu Y, Safrina O, Penna A, Roos J, Stauderman KA, Cahalan MD: Genome-wide RNAi screen of Ca(2+) influx identifies genes that regulate Ca(2+) release-activated Ca(2+) channel activity. *Proc Natl Acad Sci U S A* 2006;103:9357-9362.

- 6 Yu F, Sun L, Hubrack S, Selvaraj S, Machaca K: Intramolecular shielding maintains the ER Ca(2+)(+) sensor STIM1 in an inactive conformation. *J Cell Sci* 2013;126:2401-2410.
- 7 Zhou Y, Srinivasan P, Razavi S, Seymour S, Meraner P, Gudlur A, Stathopoulos PB, Ikura M, Rao A, Hogan PG: Initial activation of STIM1, the regulator of store-operated calcium entry. *Nat Struct Mol Biol* 2013;20:973-981.
- 8 Hirve N, Rajanikanth V, Hogan PG, Gudlur A: Coiled-Coil Formation Conveys a STIM1 Signal from ER Lumen to Cytoplasm. *Cell Rep* 2018;22:72-83.
- 9 Muik M, Fahrner M, Schindl R, Stathopoulos P, Frischauf I, Derler I, Plenk P, Lackner B, Groschner K, Ikura M, Romanin C: STIM1 couples to ORAI1 via an intramolecular transition into an extended conformation. *EMBO J* 2011;30:1678-1689.
- 10 Ma G, Wei M, He L, Liu C, Wu B, Zhang SL, Jing J, Liang X, Senes A, Tan P, Li S, Sun A, Bi Y, Zhong L, Si H, Shen Y, Li M, Lee MS, Zhou W, Wang J, et al.: Inside-out Ca(2+) signalling prompted by STIM1 conformational switch. *Nat Commun* 2015;6:7826.
- 11 Korzeniowski MK, Wisniewski E, Baird B, Holowka DA, Balla T: Molecular anatomy of the early events in STIM1 activation - oligomerization or conformational change? *J Cell Sci* 2017;130:2821-2832.
- 12 Schober R, Bonhenry D, Lunz V, Zhu J, Krizova A, Frischauf I, Fahrner M, Zhang M, Waldherr L, Schmidt T, Derler I, Stathopoulos PB, Romanin C, Etrich RH, Schindl R: Sequential activation of STIM1 links Ca(2+) with luminal domain unfolding. *Sci Signal* 2019;12:pii:eaax3194.
- 13 Liou J, Fivaz M, Inoue T, Meyer T: Live-cell imaging reveals sequential oligomerization and local plasma membrane targeting of stromal interaction molecule 1 after Ca2+ store depletion. *Proc Natl Acad Sci U S A* 2007;104:9301-9306.
- 14 Fahrner M, Muik M, Schindl R, Butorac C, Stathopoulos P, Zheng L, Jardin I, Ikura M, Romanin C: A coiled-coil clamp controls both conformation and clustering of stromal interaction molecule 1 (STIM1). *J Biol Chem* 2014;289:33231-33244.
- 15 Ercan E, Momburg F, Engel U, Temmerman K, Nickel W, Seedorf M: A conserved, lipid-mediated sorting mechanism of yeast Ist2 and mammalian STIM proteins to the peripheral ER. *Traffic* 2009;10:1802-1818.
- 16 Bhardwaj R, Muller HM, Nickel W, Seedorf M: Oligomerization and Ca2+/Calmodulin control binding of the ER Ca2+-sensors STIM1 and STIM2 to plasma membrane lipids. *Biosci Rep* 2013;33:pii:e00077.
- 17 Yuan JP, Zeng W, Dorwart MR, Choi YJ, Worley PF, Muallem S: SOAR and the polybasic STIM1 domains gate and regulate Orai channels. *Nat Cell Biol* 2009;11:337-343.
- 18 Hoth M, Penner R: Depletion of intracellular calcium stores activates a calcium current in mast cells. *Nature* 1992;355:353-356.
- 19 Zheng S, Zhou L, Ma G, Zhang T, Liu J, Li J, Nguyen NT, Zhang X, Li W, Nwokonko R, Zhou Y, Zhao F, Liu J, Huang Y, Gill DL, Wang Y: Calcium store refilling and STIM activation in STIM- and Orai-deficient cell lines. *Pflugers Arch* 2018;470:1555-1567.
- 20 Barak P, Parekh AB: Signaling through Ca(2+) Microdomains from Store-Operated CRAC Channels. *Cold Spring Harb Perspect Biol* 2019; DOI:10.1101/cshperspect.a035097.
- 21 Yeh YC, Parekh AB: CRAC Channels and Ca(2+)-Dependent Gene Expression; in Kozak JA, Putney JW, Jr. (eds): *Calcium Entry Channels in Non-Excitable Cells*. Boca Raton (FL), 2018, CRC Press/Taylor & Francis, pp 93-106.
- 22 Kar P, Nelson C, Parekh AB: Selective activation of the transcription factor NFAT1 by calcium microdomains near Ca2+ release-activated Ca2+ (CRAC) channels. *J Biol Chem* 2011;286:14795-14803.
- 23 Lunz V, Romanin C, Frischauf I: STIM1 activation of Orai1. *Cell Calcium* 2019;77:29-38.
- 24 Yeung PS, Yamashita M, Prakriya M: Molecular basis of allosteric Orai1 channel activation by STIM1. *J Physiol* 2019; DOI:10.1113/JP276550.
- 25 Brandman O, Liou J, Park WS, Meyer T: STIM2 is a feedback regulator that stabilizes basal cytosolic and endoplasmic reticulum Ca2+ levels. *Cell* 2007;131:1327-1339.
- 26 Subedi KP, Ong HL, Son GY, Liu X, Ambudkar IS: STIM2 Induces Activated Conformation of STIM1 to Control Orai1 Function in ER-PM Junctions. *Cell Rep* 2018;23:522-534.
- 27 Zweifach A, Lewis RS: Slow calcium-dependent inactivation of depletion-activated calcium current. Store-dependent and -independent mechanisms. *J Biol Chem* 1995;270:14445-14451.
- 28 Parekh AB: Slow feedback inhibition of calcium release-activated calcium current by calcium entry. *J Biol Chem* 1998;273:14925-14932.

- 29 Parekh AB: Regulation of CRAC channels by Ca(2+)-dependent inactivation. *Cell Calcium* 2017;63:20-23.
- 30 Jardin I, Albarran L, Salido GM, Lopez JJ, Sage SO, Rosado JA: Fine-tuning of store-operated calcium entry by fast and slow Ca(2+)-dependent inactivation: Involvement of SARAF. *Biochim Biophys Acta Mol Cell Res* 2018;1865:463-469.
- 31 Ng SW, Bakowski D, Nelson C, Mehta R, Almeyda R, Bates G, Parekh AB: Cysteinyl leukotriene type I receptor desensitization sustains Ca2+-dependent gene expression. *Nature* 2012;482:111-115.
- 32 Zhang X, Pathak T, Yoast R, Emrich S, Xin P, Nwokonko RM, Johnson M, Wu S, Delierneux C, Gueguinou M, Hempel N, Putney JW, Jr., Gill DL, Trebak M: A calcium/cAMP signaling loop at the ORAI1 mouth drives channel inactivation to shape NFAT induction. *Nat Commun* 2019;10:1971.
- 33 Zweifach A, Lewis RS: Rapid inactivation of depletion-activated calcium current (ICRAC) due to local calcium feedback. *J Gen Physiol* 1995;105:209-226.
- 34 Tsien RY: New calcium indicators and buffers with high selectivity against magnesium and protons: design, synthesis, and properties of prototype structures. *Biochemistry* 1980;19:2396-2404.
- 35 Gilibert JA, Parekh AB: Respiring mitochondria determine the pattern of activation and inactivation of the store-operated Ca(2+) current I(CRAC). *EMBO J* 2000;19:6401-6407.
- 36 Glitsch MD, Bakowski D, Parekh AB: Store-operated Ca2+ entry depends on mitochondrial Ca2+ uptake. *EMBO J* 2002;21:6744-6754.
- 37 Quintana A, Schwarz EC, Schwindling C, Lipp P, Kaestner L, Hoth M: Sustained activity of calcium release-activated calcium channels requires translocation of mitochondria to the plasma membrane. *J Biol Chem* 2006;281:40302-40309.
- 38 Hoth M, Button DC, Lewis RS: Mitochondrial control of calcium-channel gating: a mechanism for sustained signaling and transcriptional activation in T lymphocytes. *Proc Natl Acad Sci U S A* 2000;97:10607-10612.
- 39 Hoth M, Fanger CM, Lewis RS: Mitochondrial regulation of store-operated calcium signaling in T lymphocytes. *J Cell Biol* 1997;137:633-648.
- 40 Jha A, Ahuja M, Maleth J, Moreno CM, Yuan JP, Kim MS, Muallem S: The STIM1 CTID domain determines access of SARAF to SOAR to regulate Orai1 channel function. *J Cell Biol* 2013;202:71-79.
- 41 Palty R, Raveh A, Kaminsky I, Meller R, Reuveny E: SARAF inactivates the store operated calcium entry machinery to prevent excess calcium refilling. *Cell* 2012;149:425-438.
- 42 Albarran L, Lopez JJ, Amor NB, Martin-Cano FE, Berna-Erro A, Smani T, Salido GM, Rosado JA: Dynamic interaction of SARAF with STIM1 and Orai1 to modulate store-operated calcium entry. *Sci Rep* 2016;6:24452.
- 43 Maleth J, Choi S, Muallem S, Ahuja M: Translocation between PI(4, 5)P2-poor and PI(4, 5)P2-rich microdomains during store depletion determines STIM1 conformation and Orai1 gating. *Nat Commun* 2014;5:5843.
- 44 Derler I, Fahrner M, Muik M, Lackner B, Schindl R, Groschner K, Romanin C: A Ca2(+)-release-activated Ca2(+)- (CRAC) modulatory domain (CMD) within STIM1 mediates fast Ca2(+)-dependent inactivation of ORAI1 channels. *J Biol Chem* 2009;284:24933-24938.
- 45 Lee KP, Yuan JP, Zeng W, So I, Worley PF, Muallem S: Molecular determinants of fast Ca2+-dependent inactivation and gating of the Orai channels. *Proc Natl Acad Sci U S A* 2009;106:14687-14692.
- 46 Mullins FM, Park CY, Dolmetsch RE, Lewis RS: STIM1 and calmodulin interact with Orai1 to induce Ca2+-dependent inactivation of CRAC channels. *Proc Natl Acad Sci U S A* 2009;106:15495-15500.
- 47 Zhang M, Yuan T: Molecular mechanisms of calmodulin's functional versatility. *Biochem Cell Biol* 1998;76:313-323.
- 48 Tanaka T, Hidaka H: Hydrophobic regions function in calmodulin-enzyme(s) interactions. *J Biol Chem* 1980;255:11078-11080.
- 49 Ben-Johny M, Dick IE, Sang L, Limpitkul WB, Kang PW, Niu J, Banerjee R, Yang W, Babich JS, Issa JB, Lee SR, Namkung H, Li J, Zhang M, Yang PS, Bazzazi H, Adams PJ, Joshi-Mukherjee R, Yue DN, et al.: Towards a Unified Theory of Calmodulin Regulation (Calmodulation) of Voltage-Gated Calcium and Sodium Channels. *Curr Mol Pharmacol* 2015;8:188-205.
- 50 Urrutia J, Aguado A, Muguruza-Montero A, Nunez E, Malo C, Casis O, Villarroel A: The Crossroad of Ion Channels and Calmodulin in Disease. *Int J Mol Sci* 2019;20:pii:E400.
- 51 Singh BB, Liu X, Tang J, Zhu MX, Ambudkar IS: Calmodulin regulates Ca(2+)-dependent feedback inhibition of store-operated Ca(2+) influx by interaction with a site in the C terminus of TrpC1. *Mol Cell* 2002;9:739-750.

- 52 Singh AK, McGoldrick LL, Twomey EC, Sobolevsky AI: Mechanism of calmodulin inactivation of the calcium-selective TRP channel TRPV6. *Sci Adv* 2018;4:eaau6088.
- 53 O'Connell DJ, Bauer M, Linse S, Cahill DJ: Probing calmodulin protein-protein interactions using high-content protein arrays. *Methods Mol Biol* 2011;785:289-303.
- 54 Bauer MC, O'Connell D, Cahill DJ, Linse S: Calmodulin binding to the polybasic C-termini of STIM proteins involved in store-operated calcium entry. *Biochemistry* 2008;47:6089-6091.
- 55 Miederer AM, Alansary D, Schwar G, Lee PH, Jung M, Helms V, Niemeyer BA: A STIM2 splice variant negatively regulates store-operated calcium entry. *Nat Commun* 2015;6:6899.
- 56 Traxler L, Rathner P, Fahrner M, Stadlbauer M, Faschinger F, Charnavets T, Muller N, Romanin C, Hinterdorfer P, Gruber HJ: Detailed Evidence for an Unparalleled Interaction Mode between Calmodulin and Orai Proteins. *Angew Chem Int Ed Engl* 2017;56:15755-15759.
- 57 Frischauf I, Schindl R, Bergsmann J, Derler I, Fahrner M, Muik M, Fritsch R, Lackner B, Groschner K, Romanin C: Cooperativeness of Orai cytosolic domains tunes subtype-specific gating. *J Biol Chem* 2011;286:8577-8584.
- 58 Liu Y, Zheng X, Mueller GA, Sobhany M, DeRose EF, Zhang Y, London RE, Birnbaumer L: Crystal structure of calmodulin binding domain of orai1 in complex with Ca²⁺ calmodulin displays a unique binding mode. *J Biol Chem* 2012;287:43030-43041.
- 59 Mullins FM, Yen M, Lewis RS: Orai1 pore residues control CRAC channel inactivation independently of calmodulin. *J Gen Physiol* 2016;147:137-152.
- 60 Shen X, Valencia CA, Szostak JW, Dong B, Liu R: Scanning the human proteome for calmodulin-binding proteins. *Proc Natl Acad Sci U S A* 2005;102:5969-5974.
- 61 Li X, Wu G, Yang Y, Fu S, Liu X, Kang H, Yang X, Su XC, Shen Y: Calmodulin dissociates the STIM1-Orai1 complex and STIM1 oligomers. *Nat Commun* 2017;8:1042.
- 62 Ercan E, Chung SH, Bhardwaj R, Seedorf M: Di-Arginine Signals and the K-Rich Domain Retain the Ca(2+) Sensor STIM1 in the Endoplasmic Reticulum. *Traffic* 2012;13:992-1003.
- 63 Harmsen T, Klaasen S, van de Vrugt H, Te Riele H: DNA mismatch repair and oligonucleotide end-protection promote base-pair substitution distal from a CRISPR/Cas9-induced DNA break. *Nucleic Acid Res* 2018;46:2945-2955.
- 64 Dorr K, Kilch T, Kappel S, Alansary D, Schwar G, Niemeyer BA, Peinelt C: Cell type-specific glycosylation of Orai1 modulates store-operated Ca²⁺ entry. *Sci Signal* 2016;9:ra25.
- 65 Ikura M, Clore GM, Gronenborn AM, Zhu G, Klee CB, Bax A: Solution structure of a calmodulin-target peptide complex by multidimensional NMR. *Science* 1992;256:632-638.
- 66 Meador WE, Means AR, Quijcho FA: Target enzyme recognition by calmodulin: 2.4 Å structure of a calmodulin-peptide complex. *Science* 1992;257:1251-1255.
- 67 Meador WE, Means AR, Quijcho FA: Modulation of calmodulin plasticity in molecular recognition on the basis of x-ray structures. *Science* 1993;262:1718-1721.
- 68 Osawa M, Tokumitsu H, Swindells MB, Kurihara H, Orita M, Shibamura T, Furuya T, Ikura M: A novel target recognition revealed by calmodulin in complex with Ca²⁺-calmodulin-dependent kinase kinase. *Nat Struct Biol* 1999;6:819-824.
- 69 Yap KL, Kim J, Truong K, Sherman M, Yuan T, Ikura M: Calmodulin target database. *J Struct Funct Genomics* 2000;1:8-14.
- 70 Kilch T, Alansary D, Peglow M, Dorr K, Rychkov G, Rieger H, Peinelt C, Niemeyer BA: Mutations of the Ca²⁺-sensing stromal interaction molecule STIM1 regulate Ca²⁺ influx by altered oligomerization of STIM1 and by destabilization of the Ca²⁺ channel Orai1. *J Biol Chem* 2013;288:1653-1664.
- 71 Frischauf I, Muik M, Derler I, Bergsmann J, Fahrner M, Schindl R, Groschner K, Romanin C: Molecular determinants of the coupling between STIM1 and Orai channels: differential activation of Orai1-3 channels by a STIM1 coiled-coil mutant. *J Biol Chem* 2009;284:21696-21706.
- 72 Stathopoulos PB, Schindl R, Fahrner M, Zheng L, Gasmi-Seabrook GM, Muik M, Romanin C, Ikura M: STIM1/Orai1 coiled-coil interplay in the regulation of store-operated calcium entry. *Nat Commun* 2013;4:2963.
- 73 Wang X, Wang Y, Zhou Y, Hendron E, Mancarella S, Andrade MD, Rothberg BS, Soboloff J, Gill DL: Distinct Orai-coupling domains in STIM1 and STIM2 define the Orai-activating site. *Nat Commun* 2014;5:3183.
- 74 Thompson JL, Lai-Zhao Y, Stathopoulos PB, Grossfield A, Shuttleworth TJ: Phosphorylation-mediated structural changes within the SOAR domain of stromal interaction molecule 1 enable specific activation of distinct Orai channels. *J Biol Chem* 2018;293:3145-3155.

- 75 Calloway N, Holowka D, Baird B: A Basic Sequence in STIM1 Promotes Ca(2+) Influx by Interacting with the C-Terminal Acidic Coiled Coil of Orai1. *Biochemistry* 2010;49:1067-1071.
- 76 Korzeniowski MK, Manjarres IM, Varnai P, Balla T: Activation of STIM1-Orai1 involves an intramolecular switching mechanism. *Sci Signal* 2010;3:ra82.
- 77 Palty R, Fu Z, Isacoff EY: Sequential Steps of CRAC Channel Activation. *Cell Rep* 2017;19:1929-1939.
- 78 Monera OD, Sereda TJ, Zhou NE, Kay CM, Hodges RS: Relationship of sidechain hydrophobicity and alpha-helical propensity on the stability of the single-stranded amphipathic alpha-helix. *J Pept Sci* 1995;1:319-329.
- 79 Parvez S, Beck A, Peinelt C, Soboloff J, Lis A, Monteilh-Zoller M, Gill DL, Fleig A, Penner R: STIM2 protein mediates distinct store-dependent and store-independent modes of CRAC channel activation. *FASEB J* 2008;22:752-761.